

Characterization and Properties of Reactive Poly(lactic acid)/Polyamide 610 Biomass Blends

Fang-Cheng Pai,¹ Sun-Mou Lai,² Hou-Hsein Chu¹

¹Department of Chemical Engineering, Feng Chia University, Taichung 100, Taiwan, ROC

²Department of Chemical and Materials Engineering, National I-Lan University, I-Lan 260, Taiwan, ROC

Correspondence to: S.-M. Lai (E-mail: smlai@niu.edu.tw)

ABSTRACT: A low molecular weight bisphenol-A type epoxy resin was used as a reactive compatibilizer for poly(lactic acid) (PLA)/polyamide 610 (PA 610) biomass blends. To the best of our knowledge, this blend is the first biomass PA 610 blend in the literature. The epoxy functional groups could react with the terminal groups of both PLA and PA 610. An ester–amide interchange reaction led to a polyester–polyamide copolymer formation, and improved the compatibility of PLA and PA 610. The blends with epoxy resin showed an enhancement in the phase dispersion and interfacial adhesion compared with the blend without epoxy resin. The differential scanning calorimetry (DSC) analysis showed that the crystallization peak temperatures decreased with increasing epoxy content. The melting temperature of PA 610 decreased with the addition of PLA, but remained unchanged with increased compatibilizer dosages. The dynamic mechanical analysis (DMA) showed that the glass transition temperature (T_g) of the blend, with the addition of 0.5 phr epoxy resin, slightly increased compared with that of neat PLA. However, the T_g of the blends remained unchanged with increasing epoxy resin content, and the higher content of epoxy resin in the blends resulted in improved mechanical properties and higher melt viscosity. The unnotched impact test showed that PA 610 could toughen PLA with the addition of epoxy resin. Moreover, the no-break unnotched impact behavior was observed with the medium content of the compatibilizer, improving the notch sensitivity of PLA. © 2013 Wiley Periodicals, Inc. *J. Appl. Polym. Sci.* 130: 2563–2571, 2013

KEYWORDS: poly(lactic acid); polyamide 610; epoxy resin; compatibility; notch sensitivity

Received 7 January 2013; accepted 28 April 2013; Published online 27 May 2013

DOI: 10.1002/app.39473

INTRODUCTION

Given the current shortage of global petroleum and the steady increase in oil prices, people have started to realize to not solely rely on petroleum resource. In addition, global warming has caused serious impact on the environment; thus, the reduction of carbon dioxide emission and the exploitation of renewable energy are urgently necessary. Green biomass polymer, a renewable material, has been regarded as one of the solutions to the aforementioned problems. The ingredients or partial ingredients of these green polymers are derived from renewable resources instead of petrochemical component, and their total energy consumption and carbon dioxide emission in the life cycle assessment are less severe than that of conventional petroleum-based polymers.¹

Among these green polymers, poly(lactic acid) (PLA) could be considered as the most representative and promising biomass material because it can be easily fabricated and exhibits good mechanical properties. Numerous studies have worked on blending PLA with either biomass polymer^{2–4} or non-biomass polymer^{5–8} to improve its drawbacks and maintain its

biodegradable or biomass nature. Recently, a new biomass polymer, polyamide 610 (PA 610), has received a great deal of attention. This polymer exhibits the same properties as those of petroleum-based polyamide 610, but the sebacic acid monomer used to synthesize this polymer with hexamethylene diamine monomer is different. In this biomass polyamide 610, the sebacic acid monomer is derived from castor oil, and a share of 63% of the carbon is derived from a renewable feedstock.⁹ Castor oil is obtained from the bean of the castor oil plant, and contains a high proportion of hydroxy fatty acid, which is highly valued in the chemical industry.¹⁰ The first castor-based commercialized polyamide is polyamide 11, in which the monomer, 11-aminoundecanoic acid, is obtained from 100% castor oil.¹¹ The wide range of industrial applications of castor oil has launched various new bio-based polyamides, such as polyamide 10, polyamide 1010, polyamide 610, and so on.¹¹ Among which, polyamide 610 receives much attention because its applications cover the areas where a polymer of biological origin is considered, aside from the applications of the conventional polyamide 6 and polyamide 66.

The biomass PLA/PA 610 blend is a promising blend due to the outstanding properties of polyamide 610 in enhancing the drawbacks of amorphous PLA. However, this blend is incompatible without the addition of a compatibilizer; the blend will show deteriorated properties compared with those of neat PLA and biomass PA 610. Some studies^{12,13} working on the blends of polyester and polyamide showed a polyester–polyamide block copolymer formation, which improved the compatibility of the polymers during melt blending. Unfortunately, the mechanical properties of this blend are still poor, although the compatibility of the blend has been improved. Huang et al.¹⁴ used a low molecular weight epoxy resin as a compatibilizer to improve the compatibility of poly(ethylene terephthalate) (PET)/polyamide 6 (PA 6) blend. The notched impact strength and flexural strength of the blends were significantly improved when epoxy resin was incorporated into the blend, as a result of the reaction of the compatibilizer epoxy groups with the functional groups of both polyester and polyamide. In this study, biomass PLA/PA 610 blends were created by using a bifunctional epoxy resin as a reactive compatibilizer to improve the compatibility of PLA and biomass PA 610. To our best knowledge, this blend is the first biomass PA 610 blend in the literature. The effect of PLA used in this work on the mechanical properties, thermal properties, and morphology of the blends were also investigated.

EXPERIMENTAL

Materials

The base polymer for the blends was PLA 4060D provided by Natureworks LLC. This grade exhibited a glass transition temperature (T_g) of 56°C, a density of 1.24 g/cm³, and a melt flow rate (190°C, 2.16 kg) of 22.4 ± 0.3 g/10 min. The PA 610, with the trade name Ultramid[®] S3K Balance, was kindly supplied by Basf Co., Germany. This grade exhibited a T_m of 220°C, a density of 1.08 g/cm³, and a melt flow rate (235°C, 2.16 kg) of 33.5 ± 0.2 g/10 min. The compatibilizer used was a bisphenol-A type epoxy resin with the grade No. NPES-907L, supplied by Nan Ya Plastics, Taiwan. The epoxy equivalency was 1044 g/eq, with a softening point of 119°C.

Sample Preparations

Melt Blending. The blends were processed in a twin screw extruder (Kobe KTX-30, Japan, L/D = 43, ϕ = 30 mm) under 120 rpm of screw revolution at the temperature profile of 200–230°C. Prior to extrusion, the PLA and PA 610 were dried in an air-circulated oven at 80°C for over 24 h. The weight % of the PLA/PA 610 blends was fixed at a ratio of 50/50. Various amounts of epoxy resin at 0.5, 1, 2, 3, and 5 phr (parts per hundred resins of PLA and PA 610) were dry-blended with the PLA/PA 610 blends first, and the mixtures were fed into the twin screw extruder at a feeding rate of 12 kg/h. The pelletized compounds were dried at 80°C for over 24 h before the injection molding process.

Injection Molding. The test specimens were prepared by using an injection molding machine (VTMW VS-80H, Taiwan). The barrel temperature profile ranged from 230°C to 240°C, and the mold temperature was maintained at 30°C. The prepared blends were injection-molded into tensile, flexural, and impact specimens according to ASTM D638, D790, and D256 standards,

respectively. All the test specimens were then conditioned at 23°C and relative humidity of 50% for 24 h for further measurements.

Measurements

Morphology Analysis. The morphology of the blends was observed by using a scanning electron microscope (SEM, TESCAN 5136MM). The samples were cryo-fractured in liquid nitrogen for 10 min to obtain the fractured surfaces. The fractured samples were then coated with a thin layer of gold for SEM observation, with a magnification of 3000× under an operating voltage of 1 kV.

Structure Characterization. Fourier transform infrared (FTIR) spectroscopy (Digilab FTS3500) was performed to investigate the interaction of the epoxy group with the PLA and PA 610. The spectra were scanned with a wavelength ranging from 4000 cm⁻¹ to 400 cm⁻¹ at a resolution of 4 cm⁻¹ for 128 scans.

Mechanical Properties. The tensile test was carried out at a crosshead speed of 10 mm/min using a Universal Tensile Tester (Gotech AI-7000M). Using the same tester, the flexural test was conducted by a three-point bending method. The impact test specimens obtained from the injection-molding process were cut by a notch cutter. The Izod impact test was performed using an impact testing machine (Gotech GT-7045). Five specimens were tested for each sample to obtain an average value in all mechanical property measurement.

Thermal Analysis. A dynamic mechanical analyzer (DMA, Perkin Elmer DMA7e) was used to determine the T_g of the PLA/PA 610 blends. A three-point bending mode was used at a frequency of 1 Hz, with the temperature ranging from 0°C to 180°C, and the heating rate was 5°C/min.

Differential scanning calorimetry (DSC) measurement was performed by using a MDSC 2920 (TA Instrument). Initially, the samples were heated from room temperature to 260°C to eliminate thermal history. Samples were then cooled down to 30°C, and finally heated from 30°C to 260°C. Both of the heating and cooling rates were set at 10°C/min.

Melt Flow Rate. The melt flow rate (MFR) was measured with a load of 2.16 kg using a Gotech apparatus (GT-7100-MI) at 225°C.

RESULTS AND DISCUSSION

FTIR Observation

IR spectroscopy was used to detect the reaction of epoxy resin with PLA and PA 610, and their spectra are shown in Figure 1. Three specific peaks at 830, 1020, and 1510 cm⁻¹ were included for the characteristic absorption of the epoxy group in the epoxy resin.¹⁴ The control PLA/epoxy and PA 610/epoxy blends were also investigated. The specific peaks at 830 and 1510 cm⁻¹ became weaker, and the peak at 1020 cm⁻¹ almost disappeared, due to the interaction of the epoxy resin with PLA. In addition, an ester group peak at 1735 cm⁻¹¹⁵ for PLA shifted to 1751 cm⁻¹ for the PLA/epoxy blends. When epoxy resin reacted with PA 610, the variation of specific peaks for the epoxy group was about the same as those for the PLA/epoxy blend. The peak at 1020 cm⁻¹ was not observed, illustrating the interaction of

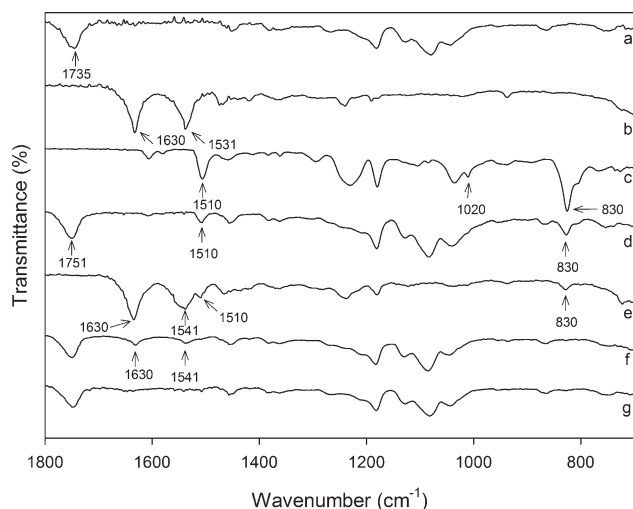


Figure 1. FTIR spectra of PLA/PA 610 blends (Expanded region): (a) neat PLA, (b) neat PA 610, (c) neat epoxy, (d) PLA/epoxy = 50/50, (e) PA 610/epoxy = 50/50, (f) PLA/PA 610/epoxy = 50/50/0 phr, and (g) PLA/PA 610/epoxy = 50/50/5 phr.

epoxy resin with PA 610. In addition, a shift was observed on the N–H bending band of PA 610 from 1531 to 1541 cm^{-1} for the PA 610/epoxy blend;¹⁴ the peak at 1541 cm^{-1} became broader.

When epoxy resin as a compatibilizer reacted with both PLA and PA 610, the three characteristic peaks of epoxy resin disappeared. These results indicated the reactions that occurred between the epoxy resin and the terminal functional group of the PLA and PA 610 in this compatibilized blend. Moreover, a carbonyl peak of PA 610 was observed at 1630 cm^{-1} ,¹³ which became weaker when PA 610 blended with PLA, and disappeared completely when PA 610 blended with both PLA and epoxy resin. This observation proved that an ester–amide interchange happened during the PLA/PA 610/epoxy reaction, which led to a polyester–polyamide block copolymer.¹³ This copolymer acted as an interfacial agent to improve the compatibility of the PLA/PA 610 blends. These results confirmed the effectiveness of epoxy as an efficient compatibilizer to PLA/PA 610 blends. Figure 2 shows the reaction scheme of the aforementioned interchange reaction.

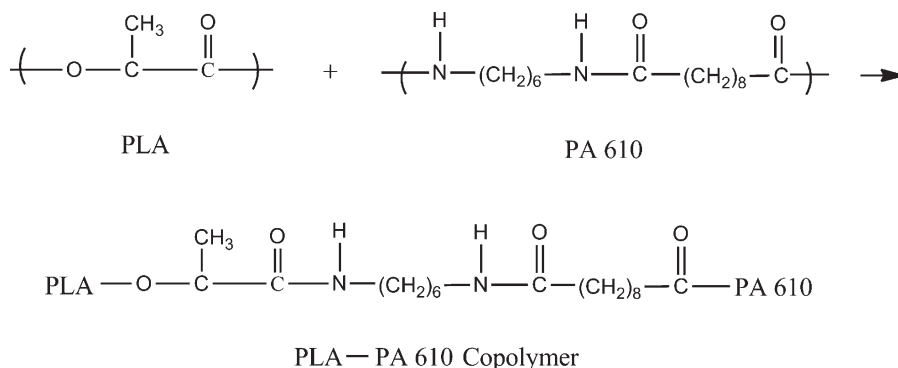


Figure 2. The reaction scheme of an ester–amide interchange reaction.

Morphology

SEM images for the fractured surface of PLA/PA 610 blends with various epoxy contents are shown in Figure 3. The PA 610 was the dispersed phase and PLA was the continuous phase, because the melt viscosity of PA 610 was much higher than that of PLA under the same condition, as determined from the MFR test (and will be discussed later). For the PLA/PA 610 blend without epoxy resin, the domain size of the dispersed PA 610 phase in the continuous PLA phase was very broad, exhibiting up to ten-fold difference. A typical morphology of the incompatible system was observed, indicating a poor dispersion of PA 610 in the PLA phase. However, the incorporation of epoxy resin to the blends resulted in remarkable changes in the domain sizes for the blends, and the adhesion between PLA and PA 610 interface was enhanced. When 0.5 phr of epoxy resin was added, the dimension of the dispersed PA 610 domains decreased, and their domain sizes were less than 3 μm . When 1 phr of epoxy resin was incorporated, smaller domain sizes and more uniform distribution was observed, in which the average domain size of the PA 610 phase was *ca.* 1 μm . However, the domain sizes of the PA 610 phase in the PLA matrix increased slightly with further increase in epoxy content, although uniform domain size distribution was retained. This result is attributed to the PA 610 agglomeration accompanied with an irregular morphology of the PLA/PA 610 blends. Sun et al.¹⁶ studied on acrylonitrile–butadiene–styrene grafted glycidyl methacrylate (ABS-*g*-GMA)-toughened PLA blends, in which 1 wt % GMA in ABS-*g*-GMA showed a much better dispersive phase morphology. Further increase of GMA content induced the agglomeration of ABS-*g*-GMA due to the crosslinking reaction between PLA and ABS-*g*-GMA. A similar study to point out the increased agglomeration with increasing GMA content was reported on ABS-*g*-GMA-toughened Nylon 6 blends.¹⁷ These results supported our findings as well. When the content of epoxy resin was low, the compatibilized reaction proceeded and improved the compatibility of the blends. However, when the content of epoxy resin was high, the crosslinking reaction may take place and induce the agglomeration of the PA 610 particles. The crosslinking reaction will interfere with the phase morphology formation when it occurs; then the dispersed particles may become viscous and less deformable.¹⁷ This result was in line with our MFR test, which will be discussed later. The MFR of the PLA/PA 610 blends decreased (i.e., viscosity increased) with increasing epoxy resin content. The additional

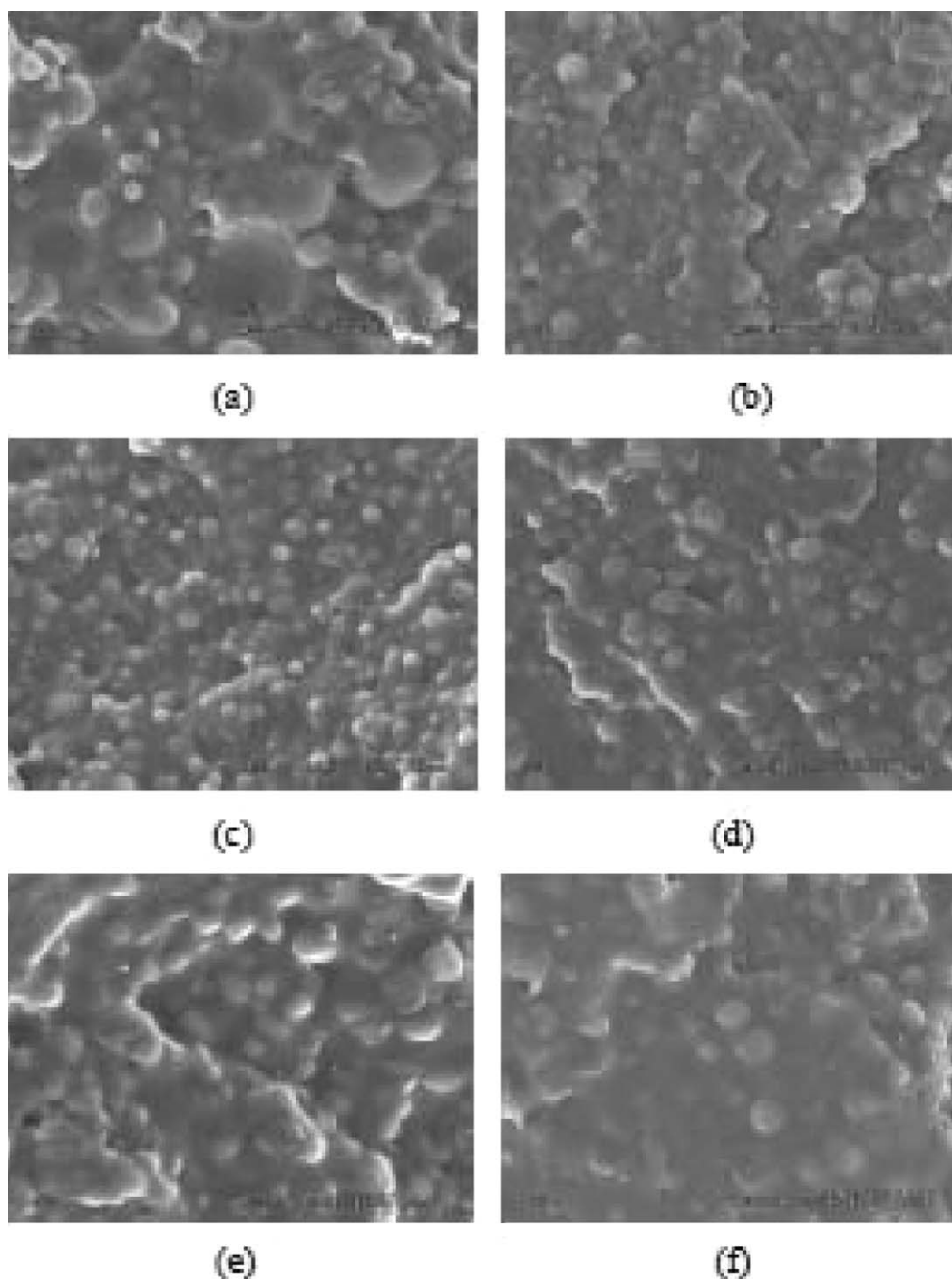


Figure 3. SEM micrographs of PLA/PA 610 blends with different ratio of epoxy resin: (a) 0 phr, (b) 0.5 phr, (c) 1 phr, (d) 2 phr, (e) 3 phr, and (f) 5 phr.

increase in the viscosity may be attributed to the increased molecular weight and the crosslinking reactions from the epoxy group with the terminal functional group of PLA and/or PA 610.

To confirm the reaction mechanism of this system, a solvent test was carried out to investigate whether or not the crosslinking reaction occurred during the melt blending of PLA and PA 610. In this study, dimethyl formamide (DMF) was used as a solvent because it could dissolve both PLA and PA 610. Figure

4 (from left to right) shows the photos of the blend solutions containing 0, 1, 3, and 5 phr of epoxy in the DMF medium. For the 0 phr case, a clear solution could be observed, which confirmed that it was an incompatible blend with no interfacial interaction between the PLA and PA 610 interface. Both the 1 and 3 phr cases showed the milky, colloidal solution. The only difference was that the solution took slightly less time to be fully dissolved in the 1 phr case than that in the 3 phr case,



Figure 4. Solvent test of PLA/PA 610 blends with different ratio of epoxy resin (from left to right, 0 phr, 1 phr, 3 phr, and 5 phr).

which was attributed to a copolymer formed *in situ* during melt blending. In addition, this dispersion still showed a suspension of the fine copolymer particles; no precipitation was observed. This copolymer acted as an interfacial agent to enhance the compatibility of the PLA/PA 610 blends, as mentioned earlier. Thus, the 3 phr epoxy-filled blend still proceeded as a compatibilized reaction of the blend. However, for the 5 phr case, this blend could not be dissolved in DMF. Moreover, the pellets were slightly swollen after being immersed in the solvent for over 24 h due to the crosslinking reaction at higher epoxy content during the melt blending. A threshold amount of epoxy resin ranging from 3 phr to 5 phr will determine the transition from the compatibilized reaction to the crosslinking reaction.

Thermal Analysis

DSC measurements were conducted to investigate the thermal and crystallization behaviors of the PLA/PA 610 blends. Figures 5 and 6 show the first cooling and second heating curves of the

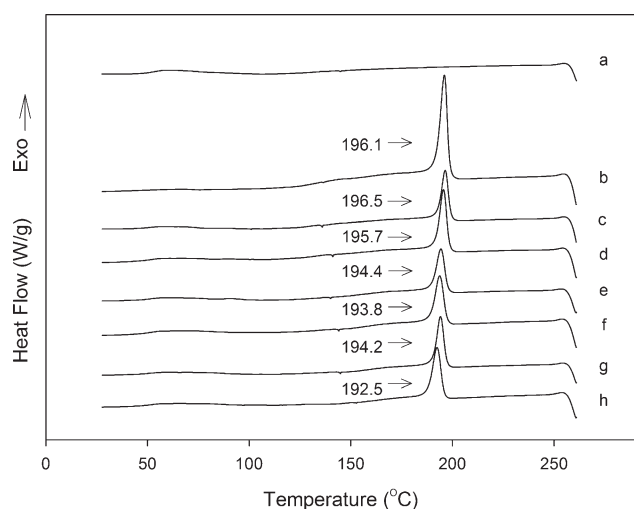


Figure 5. DSC cooling curves of neat PLA, PA 610, and PLA/PA 610 blends: (a) neat PLA, (b) neat PA 610, (c) epoxy = 0 phr, (d) epoxy = 0.5 phr, (e) epoxy = 1 phr, (f) epoxy = 2 phr, (g) epoxy = 3 phr, and (h) epoxy = 5 phr.

DSC scans for PLA, PA 610, and their blends, respectively. Table I summarizes the thermal characteristics in all cases. Figure 5 shows that the crystallization temperature of the uncompatibilized blend remained largely the same as that of PA 610. With increased compatibilizer content, the crystallization peak temperatures of the compatibilized blends were smaller than that of the neat PA 610. This difference was attributed to the presence of PLA-co-epoxy-co-PA 610 copolymers, which may hinder the PA 610 crystallization in these compatibilized blends. In addition, the crystallization exothermic peaks of the uncompatibilized and compatibilized blends were different from that of neat PA 610. Neat PA 610 showed a very sharp exothermic peak and a slightly larger value of the heat of crystallization (ΔH_c). The incorporation of PLA and the compatibilizer slightly varied the crystallization behaviors. The compatibilizer reduced the heat of crystallization of the neat PA 610. However, owing to the broad peak involved in the DSC traces, this difference in the heat of crystallization was limited.

For the melting behavior, the PLA used in our study was an amorphous polymer with no measurable melting point, but a glass transition temperature at 62.2°C, in the DSC trace, as seen in Figure 6. Also, amorphous PLA did not show any cold crystallization behavior during heating, which was different from semicrystalline PLA revealing a visible cold crystallization peak and subsequent melting peak. Meanwhile, the PA 610 was a semicrystalline polymer that showed a major and a minor melting temperature at 224.5°C (T_{m1}) and 215.2°C (T_{m2}), respectively. To the best of our knowledge, no studies have reported this interesting behavior in PA 610. However, this phenomenon was also found in a PA 610/carbon nanotube composite system, in which two melting temperatures were observed in the DSC traces.¹⁸ Sadeghi et al.¹⁹ also worked on PA 6 nanocomposites, and reported that this phenomenon was attributed to two distinct morphological species related to different forms of crystalline lamellae. These behaviors were due to the rearrangement of the lamellae, and related to lamellae thickness. The minor

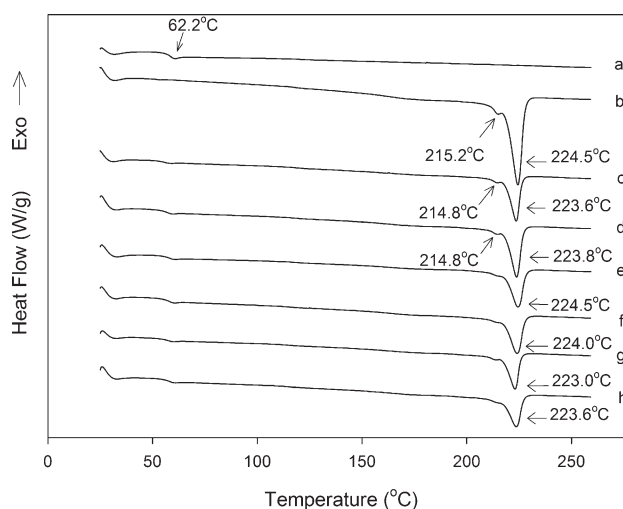


Figure 6. DSC heating curves of neat PLA, PA 610, and PLA/PA 610 blends: (a) neat PLA, (b) neat PA 610, (c) epoxy = 0 phr, (d) epoxy = 0.5 phr, (e) epoxy = 1 phr, (f) epoxy = 2 phr, (g) epoxy = 3 phr, and (h) epoxy = 5 phr.

Table I. DSC Data of PLA/PA 610 Blends

	T_c (°C)	ΔH_c (J/g)	T_{m1} (°C)	T_{m2} (°C)	ΔH_m (J/g)	X_c (%)
PLA	-	-	-	-	-	-
PA 610	196.1	46.4	224.5	215.2	48.8	24.8
PLA/PA 610/epoxy (0 phr)	196.5	45.4	223.6	214.8	47.5	24.1
PLA/PA 610/epoxy (0.5 phr)	195.7	44.6	223.8	214.8	46.1	23.4
PLA/PA 610/epoxy (1 phr)	194.4	43.6	224.5	-	44.0	22.4
PLA/PA 610/epoxy (2 phr)	193.8	43.4	224.0	-	43.0	21.9
PLA/PA 610/epoxy (3 phr)	194.2	43.8	223.0	-	42.9	21.8
PLA/PA 610/epoxy (5 phr)	192.5	42.9	223.6	-	42.2	21.4

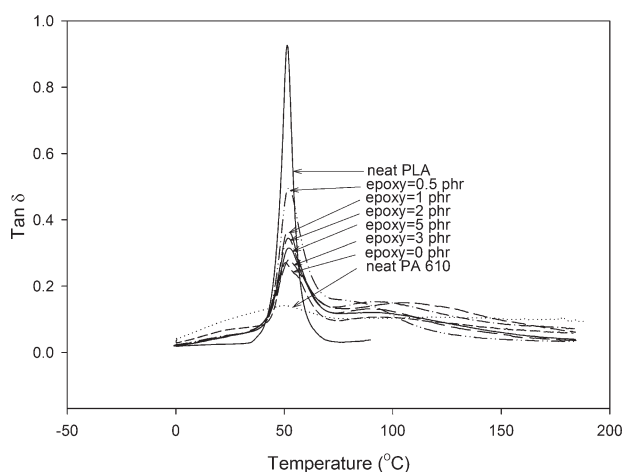
P.S.

Heat of fusion for the 100% crystalline PA 610 = 197 J/g.²⁰

Crystallinity (X_c) was calculated based on the heat of melting enthalpy.

melting temperature was associated with the thin lamellae formed during cooling, while the major melting temperature was due to the melting of the thickened lamellae during the heating or annealing process. The minor melting temperature was revealed clearly in the neat PA 610. When PLA was incorporated into the PA 610, this minor melting peak (T_{m2}) became weaker, and the peak almost disappeared when the incorporation of the quantity of the epoxy resin was above 1 phr. This observation indicated a strong hindrance of the formation of a less stable crystal form with the incorporation of epoxy resin. In Table I, the major melting temperature (T_{m1}) of PA 610 remained the same after the incorporation of epoxy resin, implying that epoxy resin had less effect on the more stable crystal of PA 610. The heat of fusion (ΔH_m) slightly decreased with increasing epoxy resin in the blends in Table I, suggesting that the crystallization of PA 610 was restrained in the presence of epoxy resin, and PA 610 had relatively lower crystallinity in the compatibilized blends than that in the uncompatibilized blend.

A dynamic mechanical analysis (DMA) was used to determine the thermal transitions and analyze the miscibility of the PLA/PA 610 blends. Figure 7 shows the $\tan \delta$ curves of PLA/PA 610 blends containing various amounts of epoxy resin. The neat PA

**Figure 7.** $\tan \delta$ spectra of PLA/PA 610 blends.

610 curve showed a very broad peak at around 48°C, which was the T_g of PA 610. Likewise, a very sharp peak was also observed at 52°C, indicating the T_g of PLA. The respective T_g s of the blends were too close, so the shift of glass transition temperature in their blend was hard to reveal. When PLA blended with PA 610 without epoxy resin, the α -peak of the blends was relatively narrower compared with other epoxy compatibilized blends, indicating limited interaction between the PLA and PA 610 interface. When 0.5 phr epoxy resin was incorporated into the PLA/PA 610 blend, the T_g of the blend slightly increased *ca.* 2°C with respect to that of neat PLA. The T_g of the blends remained unchanged with increasing epoxy resin content. However, the peak value of the compatibilized blends was relatively higher than that of the uncompatibilized blend, indicating that the incorporation of epoxy resin could increase the compatibility between PLA and PA 610 phases. Huang et al.¹⁴ worked on PET/PA 6 blends, in which the peak value of the compatibilized blend was higher than that of the uncompatibilized blend, and the peak broadening was also observed due to the higher interaction through the addition of compatibilizer. The phenomena justified our results, which revealed that the compatibility of the PLA and PA 610 phases was improved when epoxy resin was incorporated into the blend.

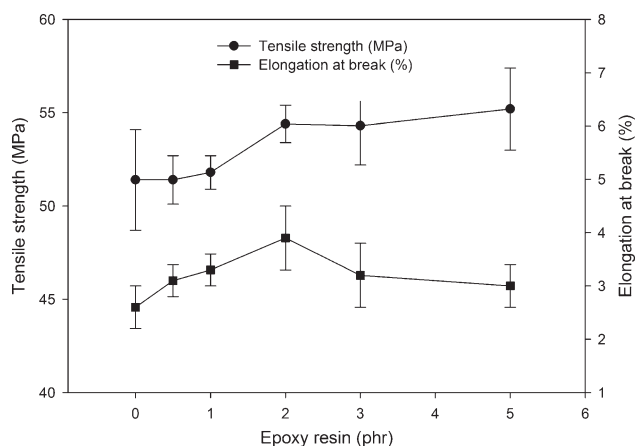
**Figure 8.** Tensile properties of PLA/PA 610 blends.

Table II. Mechanical Properties of PLA/PA 610 Blends

Compositions (epoxy ratio)	Tensile strength (MPa)	Young's modulus (MPa)	Elongation at break (%)	Flexural strength (MPa)	Flexural modulus (MPa)	Notched Impact (J/m)	Unnotched Impact (J/m)
Neat PLA	61.4 ± 0.5	2680 ± 160	5.1 ± 0.7	101.1 ± 3.0	3023 ± 25	28.4 ± 2.0	186.2 ± 2.0
Neat PA 610	54.6 ± 0.2	2082 ± 10	135 ± 8.0	84.2 ± 2.2	1853 ± 1	39.2 ± 2.9	No Break
0 phr	51.4 ± 2.7	2202 ± 85	2.6 ± 0.4	87.3 ± 3.6	2205 ± 19	11.8 ± 2.0	170.5 ± 31.4
0.5phr	51.4 ± 1.3	2325 ± 58	3.1 ± 0.3	88.1 ± 0.9	2255 ± 7	16.7 ± 3.9	167.6 ± 20.6
1 phr	51.8 ± 0.9	2276 ± 70	3.3 ± 0.3	88.3 ± 1.5	2201 ± 10	17.6 ± 2.0	385.1 ± 32.3
2 phr	54.4 ± 1.0	2301 ± 112	3.9 ± 0.6	88.7 ± 0.4	2228 ± 25	24.5 ± 4.9	No Break
3 phr	54.3 ± 2.1	2378 ± 101	3.2 ± 0.6	90.8 ± 1.0	2330 ± 30	26.5 ± 2.0	No Break
5 phr	55.2 ± 2.2	2568 ± 150	3.0 ± 0.4	91.3 ± 2.7	2324 ± 13	23.5 ± 2.0	305.8 ± 61.7

Mechanical Properties

Figure 8 shows the tensile strength, Young's modulus, and elongation at break of PLA/PA 610 blends at various epoxy resin contents, and the results are summarized in Table II. Evidently, the PLA/PA 610 blend without epoxy resin showed poor tensile properties, with the tensile strength and elongation at break ranked the lowest in all systems. This result was attributed to the lack of specific interaction between PLA and PA 610 interface, as evidenced that PA 610 could not be well-dispersed in the PLA phase from the SEM micrograph in Figure 3(a). However, the tensile properties increased with increasing the epoxy resin content. With the addition of 1 phr of epoxy resin to the system, the tensile strength and elongation at break slightly increased compared with the blend without epoxy resin. For 5 phr of epoxy resin, the tensile strength improved from 51.4 ± 2.7 to 55.2 ± 2.2 MPa, and the elongation at break slightly increased from 2.6 ± 0.4% to 3.0 ± 0.4%. This improvement was due to the increased compatibility between PLA and PA 610 through the enhanced interfacial adhesion by the reaction of epoxy group with the terminal functional group of PLA and PA 610 and the formation of a PLA-PA 610 copolymer.

The flexural strength and flexural modulus of the PLA/PA 610 blends at various epoxy resin contents are shown in Figure 9 and Table II. When PLA blended with PA 610 without epoxy resin, its flexural strength had the lowest value among all the prepared blends. Upon addition of a small amount of epoxy

resin, the degree of improvement in the flexural strength was limited. This slight improvement was similar to that of the tensile strength of the PLA/PA 610 blends. The highest enhancement was obtained when 5 phr of epoxy resin was added into the system. Compared with the blend without epoxy resin, the flexural strength improved from 87.3 ± 3.6 to 91.3 ± 2.7 MPa. This enhancement, similar to the improvement of the tensile properties of the PLA/PA 610 blends, was also attributed to the better compatibility and increased adhesion between PLA and PA 610 interface. Huang et al.¹⁴ worked on the PET/PA 6 blends by using epoxy resin E-44 as a compatibilizer. In their study, the maximum increase in flexural strength was obtained when 5 wt % E-44 was added into the blend. An et al.²¹ investigated the effect of epoxy resin E-44 on poly(butylene terephthalate) (PBT)/polyamide 6 (PA 6) blends. The appropriate E-44 content for the biggest improvement in flexural strength was between 3–6 wt %. Both of the results agreed with our study, in which 5 phr of epoxy resin improved the compatibility and adhesion of the PLA and PA 610 blends, resulting in the enhancement of flexural strength. As for the flexural modulus, a similar situation was observed with the help of an added epoxy compatibilizer. The flexural modulus for the blends increased from 2205 ± 19 MPa (0 phr epoxy) to 2324 ± 13 MPa (5 phr epoxy).

Figure 10 and Table II show the effect of epoxy resin on both notched and unnotched Izod impact strength for the PLA/PA

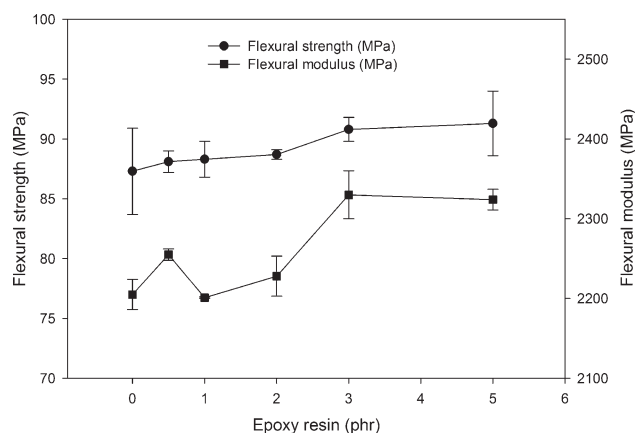


Figure 9. Flexural properties of PLA/PA 610 blends.

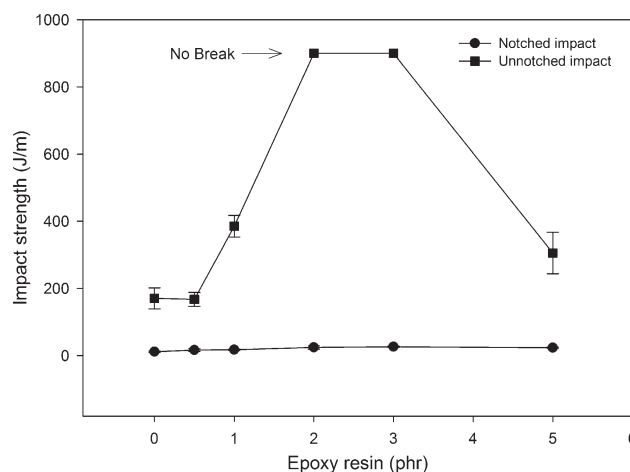


Figure 10. Izod impact strength of PLA/PA 610 blends.

610 blends. For the impact properties, neat PLA is well-known for its brittle behavior; therefore, a toughening polymer could be used to blend with PLA to enhance the PLA impact strength. PA 610, in our opinion, may be a good candidate for blending PLA to increase the PLA toughness. Surprisingly, the notched Izod impact strength of PA 610 was not as good as expected, which only showed a 39.2 ± 2.9 J/m in notched Izod impact strength. For the PLA/PA 610 blend without epoxy resin, a poor impact strength was observed, which was lower than either the PLA or PA 610. This result was due to poor compatibility between PLA and PA 610 phases. With the addition of epoxy resin into the system, the Izod impact strength was slightly increased. Although the incorporation of epoxy resin could help increase the compatibility between PLA and PA 610 interface, the degree of improvement in notched impact strength was still very limited, which was associated with typical high notch sensitivity of PLA, as discussed in our other work.²² Given that notched Izod impact test may not significantly differentiate the effect of epoxy resin content for the blends, unnotched Izod impact test was also carried out to investigate the toughness variation of these notch-sensitive blends. As expected, the unnotched impact strength increased with increased epoxy resin content. The unnotched impact strength of the blends increased dramatically from 170.5 ± 31.4 J/m (0 phr epoxy) to 385.1 ± 32.3 J/m (1 phr epoxy), which was up to 126% increment. Moreover, when either 2 phr or 3 phr epoxy resin was incorporated, the unnotched impact strength achieved no break level, representing a super tough behavior. This result revealed that epoxy resin worked as an effective compatibilizer and toughener through the enhanced adhesion between PLA and PA 610 interface. A further decrease in the unnotched impact strength at 5 phr of epoxy resin was observed, which may be attributed to the crosslinking reaction in the blend, as discussed earlier in the morphology section. The elongation at break for the blend containing 5 phr of epoxy resin showed similar trend as that of the impact strength. This result agreed with the study of Sun et al.¹⁶ who used ABS-g-GMA to toughen PLA. A small quantity of GMA within ABS-g-GMA could induce an improvement in the impact strength of the PLA blends; whereas, further increase in GMA content resulted in lower impact strength due to the crosslinking reaction. A similar paper also indicated that the crosslinking reaction at higher GMA content deteriorated the impact strength on the ABS-g-GMA-toughened Nylon 6 blends.¹⁷ These results justified our finding in the observed decrement in unnotched impact strength at higher epoxy content.

Flow Behaviors

Figure 11 shows the MFR of the incompatible and compatible PLA/PA 610 blends as a function of epoxy resin content. The highest MFR was obtained in the blend without epoxy resin, indicating that this blend exhibited the lowest melt viscosity among all the blends, which was attributed to the lack of interfacial interaction between PLA and PA 610 interface. In addition, the morphology of the SEM micrograph in Figure 3(a) showed a phase separation between PLA and PA 610 and represented an incompatible system. However, the added epoxy resin increased the melt viscosity of the blends, and therefore decreased the MFR of the blends. The higher amount of epoxy

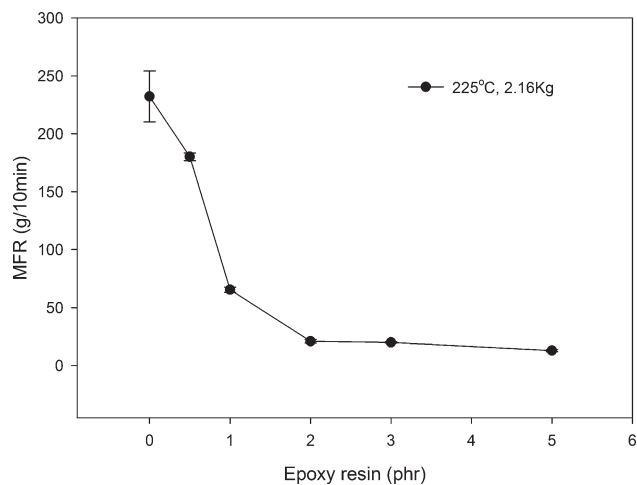


Figure 11. MFR curves of PLA/PA 610 blends.

resin was incorporated into the blends, the lower the MFR values were in the blends.

Chiou et al.²³ worked on PA 6/PBT blends using epoxy resin as a compatibilizer. In their study, epoxy resin was more compatible with PBT than with PA. Thus, it was expected that epoxy resin was more compatible with PLA than with PA 610 in our blends. Moreover, PLA had a lower melting temperature than PA 610. Hence, in the early stage of the melt blending, epoxy resin will reside mainly in the PLA phase and react with the PLA end groups, followed by the coupling reaction between the epoxy resin and PA 610 terminal groups within the interface. Therefore, an *in situ* PLA-PA 610 copolymer formed to reduce the interfacial tension between PLA and PA 610 interfaces was expected. The significant decrease of MFR in PLA/PA 610 blends suggested that epoxy resin had a crucial role as an interfacial agent to enhance the compatibility of the blends. Moreover, the MFR showed an additional gradual decrease from 20.0 ± 0.8 g/10 min at 3 phr epoxy content to 13.0 ± 0.9 g/10 min at 5 phr epoxy content, as shown in Figure 11. This result could be attributed to the crosslinking effect that caused the melt viscosity to increase in the blends. An et al.²¹ worked on PBT/PA 6 blends and found that a small amount of epoxy resin in the blend will result in the gelation of PA 6. With increased amount of epoxy resin, the crosslink intensity of PA 6 increased. These results were basically in accordance with the findings in our solvent test, as discussed in the morphology section earlier. Therefore, in our PLA/PA 610 blends, a low quantity of epoxy resin will assist the compatibilized reaction inducing the formation of copolymer in the interface, resulting in finer domains and smaller MFR values. However, when the amount of epoxy resin increased over 3 phr in the blends, it may induce the crosslinking reaction and the agglomeration of the dispersed phase, leading to decreased MFR values.

CONCLUSION

This study showed that a low molecular weight epoxy resin has a significant role as an effective reactive compatibilizer in the PLA/PA 610 blends. To our best knowledge, this blend is the first biomass PA 610 blend in the literature. The epoxy compatibilizer in the blends could react with both the terminal

functional groups of PLA and PA 610 to form the PLA-co-epoxy-co-PA 610 copolymer at the interface. This *in situ* formed copolymer tended to reduce the interfacial tension and enhance the interfacial adhesion. Therefore, the domain size of the compatibilized blends could be reduced and physical properties could be improved. Moreover, the chemical reaction during the melt blending comprised two substantial reaction mechanisms. When the amount of epoxy resin was low, the compatibilized reactions induced the formation of copolymer in the interface of the two polymers, resulting in finer domains and higher melt viscosity, as well as improved physical properties. When the amount of epoxy resin was above a critical level, a crosslinking reaction may happen, which interfered with the dispersion of the PA 610 phase due to the increased viscosity (lower melt flow rate), and led to deteriorated impact strength. Therefore, the biomass PLA/PA 610 blend would be a promising blend due to the outstanding properties of polyamide 610 at an optimum level of the compatibilizer to enhance the drawbacks of PLA in terms of environmental concerns.

ACKNOWLEDGMENTS

The authors would like to thank the Plastics Industry Development Center, Taiwan, ROC, and Prowin Tech. Plastic Co. Ltd., Taiwan, ROC, for their great assistance in the experiments.

REFERENCES

1. Su, Z.; Li, Q.; Liu, Y.; Hu, G.-H.; Wu, C. *Eur. Polym. J.* **2009**, *45*, 2428.
2. Han, L.; Han, C.; Zhang, H.; Chen, S.; Dong, L. *Polym. Compos.* **2012**, *33*, 850.
3. Harada, M.; Iida, K.; Okamoto, K.; Hayashi, H.; Hirano, K. *Polym. Eng. Sci.* **2008**, *48*, 1359.
4. Harada, M.; Ohya, T.; Iida, K.; Hayashi, H.; Hirano, K.; Fukuda, H. *J. Appl. Polym. Sci.* **2007**, *106*, 1813.
5. Wang, Y.; Chiao, S. M.; Hung, T.-F.; Yang, S.-Y. *J. Appl. Polym. Sci.* **2012**, *125*, 402.
6. Acar, I.; Durmus, A.; Ozgumus, S. *J. Appl. Polym. Sci.* **2007**, *106*, 4180.
7. Li, Y.; Shimizu, H. *Eur. Polym. J.* **2009**, *45*, 738.
8. Ran, X.; Jia, Z.; Han, C.; Yang, Y.; Dong, L. *J. Appl. Polym. Sci.* **2010**, *116*, 2050.
9. Ultramid[®] Balance Flyer, Basf. SE. Germany.
10. Mutlu, H.; Meier, M. A. R. *Eur. J. Lipid Sci. Technol.* **2010**, *112*, 10.
11. Marchildon, K. *Macromol. React. Eng.* **2011**, *5*, 22.
12. John, J.; Bhattacharya, M. *Polym. Int.* **2000**, *49*, 860.
13. Retolaza, A.; Eguiazabal, J. I.; Nazabal, J. *Polym. Eng. Sci.* **2004**, *44*, 1405.
14. Huang, Y.; Liu, Y.; Zhao, C. *J. Appl. Polym. Sci.* **1998**, *69*, 1505.
15. Zhang, J.; Li, G.; Su, Y.; Qi, R.; Ye, D.; Yu, J.; Huang, S. *J. Appl. Polym. Sci.* **2012**, *123*, 2996.
16. Sun, S.; Zhang, M.; Zhang, H.; Zhang, X. *J. Appl. Polym. Sci.* **2011**, *122*, 2992.
17. Sun, S. L.; Tan, Z. Y.; Xu, X. F.; Zhou, C.; Ao, Y. H.; Zhang, H. X. *J. Polym. Sci. Part B: Polym. Phys.* **2005**, *43*, 2170.
18. Jeong, J.-Y.; Lee, H.-J.; Kang, S.-W.; Tan, L.-S.; Baek, J.-B. *J. Polym. Sci. Part A: Polym. Chem.* **2008**, *46*, 6041.
19. Sadeghi, F.; Fereydoon, M.; Ajji, A. *Adv. Polym. Tech.* **2011**, *00*, 1.
20. Elzein, T.; Brogly, M.; Schultz, J. *Polymer* **2002**, *43*, 4811.
21. An, J.; Ge, J.; Liu, Y. *J. Appl. Polym. Sci.* **1996**, *60*, 1803.
22. Pai, F.-C.; Chu, H.-H.; Lai, S.-M. *J. Polym. Eng.* **2011**, *31*, 463.
23. Chiou, K.-C.; Chang, F.-C. *J. Polym. Sci. Part B: Polym. Phys.* **2000**, *38*, 23.